Hydration, Dynamics, and Transport across the Phase Diagram of Aqueous Poly(ethylene oxide)-*b*-poly(propylene oxide)-*b*-poly(ethylene oxide) (Pluronic L64) by Spin Probe Electron Spin Resonance and Electron Spin Resonance Imaging

Karen Malka[†] and Shulamith Schlick*

Department of Chemistry, University of Detroit Mercy, Detroit, Michigan 48219

Received September 6, 1996; Revised Manuscript Received November 22, 1996[⊗]

ABSTRACT: The aggregation of the triblock copolymer poly(ethylene oxide)-*b*-poly(propylene oxide)-*b*-poly(ethylene oxide) ($EO_{13}PO_{30}EO_{13}$; commercial name Pluronic L64) in aqueous solutions and the hydration of the PEO blocks were deduced from ESR spectra of the nitroxide spin probe perdeuterio-2,2′,6,6′-tetramethylpiperidone *N*-oxide in the temperature range 293−330 K. The isotropic ^{14}N hyperfine splitting of the nitroxide, a_N, is a key parameter that reflects the local polarity, and its variation with temperature and polymer concentration is an indicator of aggregation. The effective hydration of the polymer chains was determined by comparison of a_N values of the probe across the phase diagram with "calibration" curves of a_N in pure PEO, pure PPO, and mixtures of the homopolymers, measured as a function of the water content Z_w, where Z_w is the number of water molecules per monomer unit. The calibration curves indicated that the spin probe is preferentially located in the vicinity of the EO segments and reports on the local polarity and hydration of these segments. The *effective* degree of hydration, $Z_{w,eff}$, determined from the calibration curves and the a_N values of the probes in the L64 aqueous solutions, decreases with increase in L64 content and is significantly lower than the *average* value deduced on the basis of the water content. The dramatic drop in $Z_{w,eff}$ at 300 K, from $Z_{w,eff} \approx 23$ in 10% (w/w) L64 to $Z_{w,eff} \approx 7$ in 20% (w/w) L64, was taken as an indicator of micellization. The dependence of a_N and τ_c, the rotational correlation time of the probe, on temperature and L64 content are additional parameters that describe the local polarity and the micellization process. A superposition of two ESR signals is suggested by the line shapes detected at high polymer contents (≥90% (w/w) L64); we proposed that in these conditions the driving force for separation of the EO and PO blocks is weak, and the probe is incapable of selecting a preferred site. The translational diffusion of the spin probe was measured by ESR imaging in the L64 solutions containing 10−100% (w/w) polymer. The diffusion coefficients *D* of the spin probe decrease with increase in the polymer content, but the decrease is more prominent for L64 contents in the range 10−30% (w/w). At a polymer content of 90% (w/w), *D* is similar to that of the polymer chains (determined by field gradient NMR). We suggested that water provides an important pathway for the translational diffusion of the probe.

Introduction

Self-assembling of surfactants in aqueous solutions is a fascinating recent area of research. The hydrophobic interactions provide the driving force for the aggregation of the surfactants into micelles, liquid crystalline phases, and reverse micelles in the presence of water or mixed solvents. The type of organization and the curvature of the aggregates depend critically on the "packing" parameter v/a_0l_c, where v is the volume of the surfactant, l_c its length, and a_0 the area of the head group.[1] Spherical and rodlike micelles, bilayers, lamellar phases, and reverse micelles are formed as the geometry of the surfactant varies from a cone to a truncated cone, a cylinder, and an inverted truncated cone ("wedge"). In common ionic surfactants such as sodium dodecyl sulfate (SDS), the mean curvature of the aggregates can be varied by addition of cosurfactants or electrolytes. Study of self-assembling in these systems is complicated by the presence of additives and by the multiple types of interactions.

The nonionic water-soluble polymeric surfactants consisting of poly(ethylene oxide) (PEO) and poly(propylene oxide) (PPO) segments, Chart 1, are commercially available as triblocks PEO−PPO−PEO in a range of molecular masses and ratios of the two components and are used in diverse applications such as detergents, stabilizers, emulsifiers, cosmetics, drug release, treatment of burns, and water purification; their low toxicity is essential for the medical applications. The block copolymers, made by BASF ("Pluronics") and ICI ("Poloxamers"), are also available as triblocks PPO−PEO−PPO ("reverse Pluronics") or in a dendrimer architecture with PEO−PPO or PPO−PEO segments linked to an ethylenediamine core.[2]

Chart 1. PEO−PPO−PEO Triblock Copolymers

$$HO[\text{-}CH_2CH_2O\text{-}]_m[\text{-}CH(CH_3)CH_2O\text{-}]_n[\text{-}CH_2CH_2O\text{-}]_mH$$

$$(EO_mPO_nEO_m)$$

The most characteristic property of the Pluronic diols is the *inverse* temperature dependence of the critical micelle concentration (cmc): the cmc decreases as the temperature increases.[3,4] Interesting rheological properties follow, and gel phases are formed in some Pluronics with increase in temperature, due to the growth of the micelles and interpenetration of their coronas. This behavior has been successfully modeled by Karlström et al.,[5] Linse,[6] and Hurter et al.,[7] based on the analysis of the chain conformations expected for polymers containing the $\text{-}CH_2CH_2O\text{-}$ group: trans and gauche sequences lead to polar or nonpolar conformations, and the number of the nonpolar conformers

* To whom all correspondence should be addressed. E-mail: schlicks@udmercy. edu.

[†] Present address: Université de Poitiers, Faculté des Sciences, Bâtiment de Chimie, 40, Avenue du Recteur Pineau, 86022 Poitiers Cedex, France.

[⊗] Abstract published in *Advance ACS Abstracts,* January 15, 1997.

S0024-9297(96)01321-6 CCC: $14.00

increases with temperature. The less favorable interactions with water lead to "shrinkage" of the exterior block (PEO) exposed to water. As expected intuitively, calculations show that the interior of the micelles is primarily composed of PO units, and the corona is primarily EO. Phase diagrams predicted by this approach are in reasonable agreement with the experiment, especially for Pluronics with a relatively simple phase diagram, which includes spherical and elongated micelles at low temperatures and phase separation at higher temperatures.[6] The actual cmc values are still debated, and a recent study has suggested that the concept of limiting aggregation concentration (LAC) is more appropriate than cmc for explaining the *gradual* changes in physical properties such as surface tension and fluorescence over a range of concentrations.[8] The Pluronics have been investigated by a variety of experimental methods, including viscometry, light scattering, nuclear magnetic resonance (NMR), phase diagram determination, gelation mechanism, UV−VIS absorption of selected probes, surface tension, and fluorescence.[3,4,8−14]

Many of the experimental and theoretical studies on Pluronics have focused on the formation of micellar phases and on the micelle structure.[3,4] The calculations have clearly suggested large variations of the packing shape of the surfactants due to temperature changes: for $EO_{37}PO_{56}EO_{37}$ (P105), the area of the hydrophilic EO block at cmc is ≈430 Å^2 at 315 K and only 160 Å^2 at the transition from the rodlike micelles to the two-phase region at 335 K.[7] This modulation of the polar head size manifests itself in the rich phase diagram of some Pluronics. A case in point is the phase diagram of aqueous solutions of $EO_{13}PO_{30}EO_{13}$ (L64) in the temperature range 289−358 K, which includes spherical and elongated micellar phases (L_1 and H) as well as lamellar (L_α) and reverse micellar (L_2) phases in a wide range of temperatures and concentrations.[15] The phase diagram at 298 K of the ternary system L64/water/*p*-xylene has also been determined recently.[16] Small regions in the phase diagram of L64 suggest the presence of the bicontinuous ("sponge") cubic phase, with water regions separated by polymer bilayers.[17] Sponge phases are expected in Pluronics with a low EO content (<50% (w/w)) and with an intermediate molecular mass; higher molecular masses favor the formation of gel phases due to an increase in micelle size with temperature and to intertwining of the outside PEO blocks, and larger EO blocks do not possess the packing factor necessary for the formation of lamellar, sponge, and reverse micellar phases.[18]

We have initiated a study on Pluronics using electron spin resonance (ESR) spectroscopy of nitroxide spin probe as a source of structural and dynamical data, ESR imaging (ESRI) for measurements of the translational diffusion coefficients of the probes, and rheological measurements for a rapid evaluation of the *macro*scopic properties. The ESR measurements are based on nitroxide spin probes that vary in size, charge, hydrophilicity, and position of the nitroxide group relative to the probe head group. The specific objectives of our studies are to provide information on the local hydration and dynamics of the self-assembled system, assess the polarity profile in the various self-assembled structures, measure transport properties of the probes, evaluate the amount and nature of structural defects in the organized aggregates, and determine the effect of wedge-shaped additives such as cholesterol on the stability and structure of the lamellar, sponge, and reverse micellar phases.

Chart 2. Nitroxide Spin Probe Perdeuterio-2,2′,6,6′-tetramethylpiperidone *N*-Oxide (PDTEMPONE)

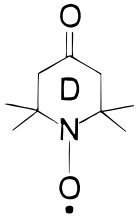

We present a study of L64 across the phase diagram in the temperature range 293−330 K, using the spin probe perdeuterio-2,2′,6,6′-tetramethylpiperidone *N*-oxide (PDTEMPONE; Chart 2). The use of a perdeuteriated spin probe allows the best *spectral* resolution and therefore the most accurate determination of magnetic and dynamic parameters, as well as the optimum *spatial* resolution in the ESRI experiments. Preliminary results for the binary system L64/water based on amphiphilic spin probes have been published,[19] and the study of the reverse micellar phase in the system L64/water/*o*-xylene with cationic spin probes has been submitted for publication.[20]

Experimental Section

Materials. The Pluronic L64 of formula $EO_{13}PO_{30}EO_{13}$ and molecular weight (MW) 2900 was a gift from BASF Corp., Wyandotte, MI. Two poly(ethylene oxide) (PEO) samples were a gift from Union Carbide: Carbowax 300 (MW = 285−315, ≈6 EO units/chain) and Carbowax 600 (MW = 600, ≈13 EO units/chain). Poly(propylene oxide) (PPO), trade name PPG 425 (MW = 425, ≈7 PO units/chain), was a gift from Arco Chemical Co. The homopolymers were dehydrated on molecular sieves (M544) from Davison (type 13-x, pore size 10 Å) and kept in a glovebox under nitrogen. The perdeuteriated spin probe PDTEMPONE (MW = 170) was synthesized according to a published procedure.[21]

Sample Preparation. Aqueous solutions of L64 were prepared under nitrogen by weighing appropriate amounts of polymer and water in 8 mm i.d. glass tubes, which were rapidly flame-sealed and centrifuged for several hours per day during 1 week to facilitate mixing.[15] The spin probe PDTEMPONE was dissolved in ethanol to a concentration of ≈10 mM and divided into several vials.[22] After evaporation of the solvent under a nitrogen stream, the two kinds of PDTEMPONE/L64/water solutions described below were prepared. All samples were prepared under nitrogen in a glovebox in order to eliminate the dissolved oxygen, which was found to broaden the ESR signals from the spin probe. The water used for preparing the L64/water solutions was flushed for 2 h with a nitrogen stream in order to minimize the concentration of oxygen.

(a) For the ESR measurements, L64/water solutions with low PDTEMPONE concentrations (≈1 mM) were prepared, in order to avoid line width broadening due to spin-spin interactions. These concentrations corresponded to a ratio [spin probe]/[monomer] of 5×10^{-4}−6×10^{-6}. The PDTEMPONE/L64/water solutions were kept under nitrogen at room temperature and then transferred under nitrogen to capillary tubes (Pasteur pipets, Fisher Brand, i.d. <1 mm) and rapidly sealed. A similar procedure was adopted for the preparation of the spin probe in aqueous solutions of PEO, PPO, and PEO/PPO mixtures.

(b) For the study of the translational diffusion by ESR imaging, higher PDTEMPONE concentrations (≈40 mM) were used, for a good ratio of signal to noise. The sample configuration and the steps of sample preparation for the diffusion experiments are described in Figure 1: The L64/water solution was introduced with a syringe to a length $l \approx 7$ mm into a

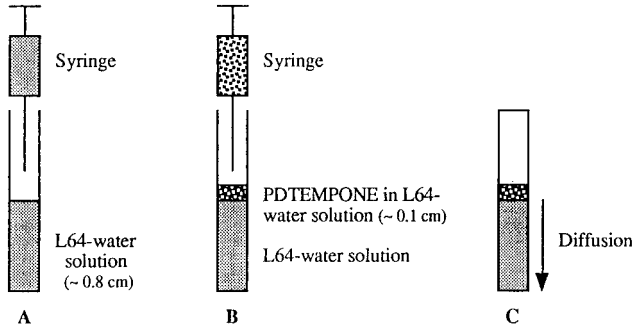

Figure 1. Three stages in sample preparation for the measurement of the translational diffusion of PDTEMPONE by ESR imaging (ESRI), as explained in the text.

glass tube (i.d. 1−1.5 mm for the L64/water solutions with L64 content of 20−100% (w/w)) (step A). In step B, the same L64/water solution also containing the spin probe was carefully placed with a syringe on top of the L64/water solution. The total length of the sample was ≈8 mm. The tube was flame-sealed (step C) to avoid loss of solvent.

ESR Measurements. ESR spectra were measured with the X-band Bruker spectrometer Model ECS106 equipped with the ESP 3240 data system for acquisition and manipulation and with the ER4111 VT variable temperature unit. Spectra were measured with 100 kHz magnetic field modulation, microwave power 2 mW, microwave frequency ≈9.4 GHz, and modulation amplitude 0.2 G. All spectra were normalized at the microwave frequency (≈9.4453 GHz) of the ESR spectrum of PDTEMPONE in water at 300 K.

ESR Imaging and Data Acquisition. The ESR imaging system consists of the Bruker 200D ESR spectrometer equipped with two Lewis coils (George Associates, Berkeley, CA, type 503D), and two regulated DC power supplies (Kikusui Electronic Corp. Japan, Model PAE 35-30). The two coils, each consisting of a figure-eight coil, are fixed on the poles of the spectrometer magnet and provide a maximum linear field gradient of ≈320 G/cm in the direction parallel to the external magnetic field (z axis) or ≈250 G/cm in the vertical direction (along the long axis, x, of the microwave cavity), with a control voltage of 20 V applied to each power supply. The magnetic field gradient was measured by recording ESR spectra of a DPPH sample, which consisted of two small specks of DPPH fixed at a distance of 1 cm along the direction of the gradient on the surface of a quartz tube (10 mm o.d.), in a range of gradients generated with control voltages ranging from 1 to 20 V; good linearity was detected for gradients along the x or z axis. The coils were positioned so that the zero point of the gradient field coincided with the center of the microwave cavity.[23]

The progress of diffusion was followed from spatial−spectral images measured as a function of time. Each image was reconstructed from a complete set of projections collected as a function of the magnetic field gradient, using a convoluted back-projection algorithm.[24] The number of points for each projection (4096) was kept constant. For a spectral width ΔH = 50 G, sample length l = 0.8 cm, and maximum field gradient of ≈200 G/cm along the vertical axis, the magnetic field sweep varied from 71 to 291 G. In practice, the magnetic field sweep of the spectrometer was initially set at the maximum sweep, and the imaging software then selected a sweep appropriate for the magnitude of the gradient used to collect data for a given projection. The number of projections was 65. Of these projections, typically 55 were experimentally accessible; the 10 projections at the "missing angles"[25] were assumed identical with those recorded at the largest experimentally accessible angle α_{max}. Each projection required one scan for an acceptable signal/noise and was collected with scan time 10 s, microwave power 2 mW, modulation 1 G, and time constant 10 ms; the spectrometer gain was 4000−10 000 in most cases. The total time required for an image was ≈20 min; this time includes the "reset" time, ≈10 ms, of the spectrometer after each projection. The tacit assumption in the imaging experiments is that the progress of diffusion can be neglected during data acquisition; this assumption is justified for the slow transport rates measured in this study.

The first-derivative ESR spectra measured in the presence of gradients were numerically integrated and multiplied by the square of the sweep width, in order to obtain a constant integrated intensity, as required by the image reconstruction algorithm; the 4096 points collected for each spectrum were compressed by averaging to 256 points. The reconstruction algorithm produced a three-dimensional spatial−spectral−intensity image of the diffusant distribution in the sample consisting of 256 × 256 points. The concentration of the diffusant at each point of the spatial axis of a sample at a given time was obtained by integrating the ESR spectra at this point along the spectral (magnetic field) axis, thus providing the corresponding experimental concentration profile. Additional experimental details have been published.[23,26−28]

Simulation of Diffusion Profiles. All experimental profiles taken for a particular sample at different times were splined using a cubic spline with 16 control points, and the part of the profiles corresponding to the sample length was selected. The diffusion coefficients were determined by comparing the experimental splined concentration profiles with calculated profiles based on Fick's laws of diffusion,[29] using the solution of the diffusion equation appropriate for the sample configuration used in our experimental setup.[23,26−28] For each time-dependent concentration profile, 21 equally spaced points were calculated. The sensitivity profile of the ESR cavity along the vertical direction was taken in consideration by multiplying the simulated profiles by the final experimental profile, measured for the **same** sample when a homogeneous distribution of the diffusant in the sample was reached. Typical times needed to attain equilibrium profiles at 300 K were 1, 3, 7, 11, 28, and 16 days for 20%, 40%, 50%, 70%, and 90% (w/w) L64 and pure L64, respectively. The time needed to reach an equilibrium probe concentration across the sample depends on the length of the sample, l, and the initial thickness of the diffusant, h. The parameters D (the diffusion coefficient) and C_0 (the total spin probe concentration) were varied for each experimental profile, until the best fit was reached; the h value was kept constant. The maximum limits of C_0 used for simulating a given system were ±13%.

From each simulated concentration profile, a value for the diffusion coefficient D was obtained. The number of D values for a given system was therefore equal to the number of images, typically 6−10. The average variation of the diffusion coefficients was ±25%, based on at least two samples studied for each L64 content.

Results

ESR Spectra of PDTEMPONE in Aqueous L64, PEO, and PPO Systems at 300 K. X-band ESR spectra at 300 K of PDTEMPONE for the indicated polymer concentration in % (w/w) are presented in Figure 2. The spectra correspond to the phases indicated in the phase diagram, Figure 3:[15] L_1 (20% (w/w)), H (50% (w/w)), L_α (70% (w/w)), and L_2 (90% (w/w)). All spectra consist of three narrow lines typical of fast dynamical averaging. The line widths, however, vary with L64 content; the line width of the center signal changes from 0.36 G for the 10% (w/w) L64 solution to 0.63 G in the 90% (w/w) L64 solution. Broad shoulders indicated by arrows are observed for the two lower spectra in Figure 2, suggesting an additional spectral component with broader lines. The isotropic ^{14}N hyperfine splitting a_N gradually decreases from a maximum value of 16.05 G in neat water to 14.66 G in neat L64 (Figure 4 and Table 1), suggesting that the local polarity at the probe site decreases with increasing polymer concentration. The experimental error in the a_N values is ±0.03 G.

In order to correlate the variation of a_N in L64/water to the degree of local hydration of the monomer seg-

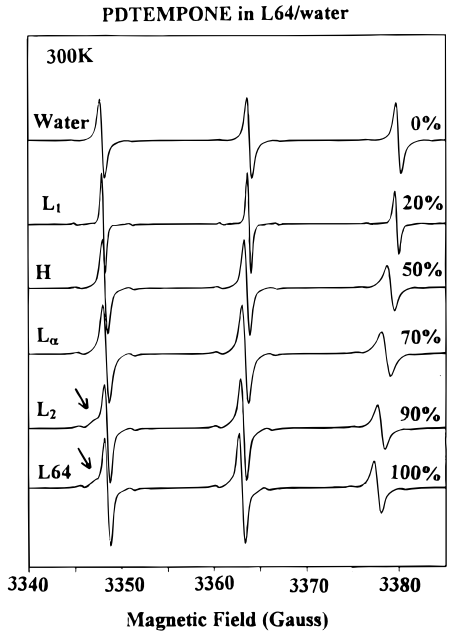

Figure 2. X-band ESR spectra at 300 K of the PDTEMPONE spin probe for the indicated L64 contents (in % (w/w)). The corresponding phases are given to the left of the spectra. Arrows in the two lower spectra indicate an additional spectral component with broader lines.

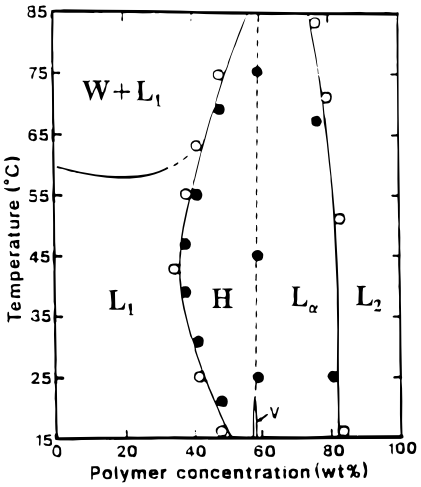

Figure 3. Phase diagram for aqueous $EO_{13}PO_{30}EO_{13}$ (Pluronic L64). L_1 and L_2 are isotropic phases, H is the hexagonal phase, L_α is the lamellar phase, and V is the cubic crystalline phase (redrawn from ref 15).

ments, we measured a_N values at 300 K of the same spin probe in PEO (Carbowax 300) and PPO (PPG425) as a function of the amount of water expressed as Z_w (number of water molecules per monomer unit); the results are shown in Figure 5. The expected lack of aggregation in the solutions of the homopolymers PEO and PPO ensures that the amount of water per monomer unit represents also the effective hydration sensed by the probe. The a_N values vary from 16.05 G in neat water to 14.90 G in pure PEO[30] and to 14.72 G in pure PPO. The different a_N values of the probe in PEO and PPO given in Figure 5 suggest that the probe is sensitive to the local polarity. In order to ascertain the probe location in greater detail, the ESR spectra of PDTEMPONE at 300 K were also measured in a *mixture* of PEO and PPO aqueous solutions corresponding to a molar ratio [EO]/[PO] = 26/30, as in L64. The splitting constant a_N in these PEO/PPO/water solutions is also shown in Figure 5 and varies from 16.05 G in

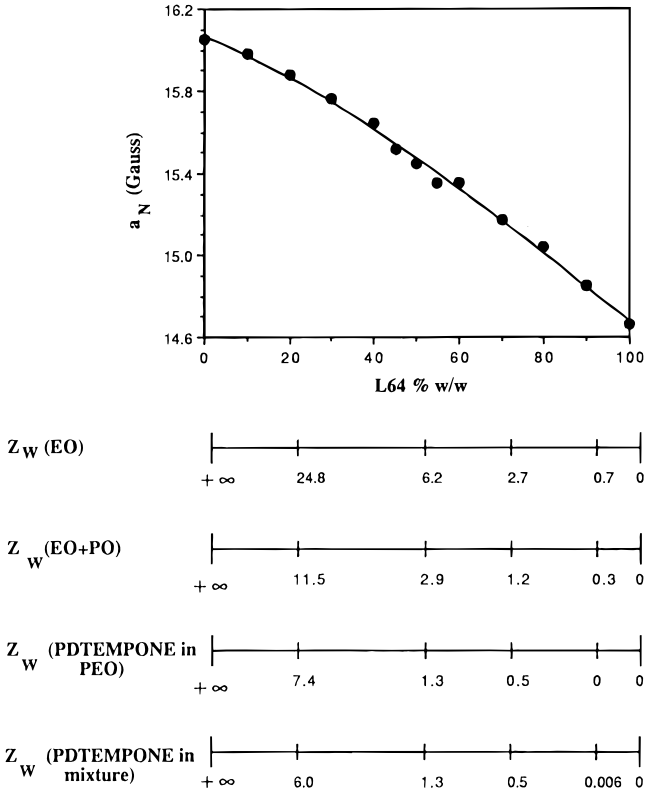

Figure 4. Variation of a_N, the ^{14}N isotropic hyperfine splitting in PDTEMPONE, at 300 K as a function of the L64 concentration in % (w/w); the experimental points are connected as a guide to the eye. The additional horizontal scales represent, from top to bottom: Z_w(EO), the number of water molecules per monomer unit in the L64 solutions, calculated by assuming that the water is associated with the EO units only; Z_w(EO + PO), the number of water molecules per monomer unit in the L64 solutions, calculated by assuming that the water is associated with the EO *and* PO units; Z_w(PDTEMPONE in PEO), the effective number of water molecules per EO unit, measured from the calibration curve based on aqueous Carbowax 300 (Figure 5); Z_w(PDTEMPONE in mixture), the number of water molecules per EO unit, measured from the calibration curve based on the aqueous PEO/PPO mixtures. The last two scales are the same within the experimental error (see text).

Table 1. Hyperfine Splitting Constants a_N (G) of PDTEMPONE in L64 Aqueous Solutions

% (w/w) L64	293 K	300 K	310 K	320 K	330 K
0	16.05	16.05	16.05	16.05	16.05
10	16.00	15.98	15.95	15.91	15.89
20	15.87	15.88	15.78	15.73	15.68
30	15.82	15.76	15.69	15.62	15.57
40	15.69	15.64	15.56	15.51	15.45
50	15.55	15.45	15.43	15.38	1.34
55	15.41	15.35	15.32	15.28	15.24
60	15.39	1.35	15.30	15.26	15.25
70	15.21	15.17	15.15	15.14	15.13
80	15.05	15.04	15.04	15.04	15.05
90	14.82	14.85	14.84	14.86	14.88
100	14.64	14.66	14.66	14.69	14.68

neat water to 14.84 G in the mixture of the homopolymers. Within experimental error, the a_N variations with water content for the spin probe in PEO and the PEO/PPO mixture are identical. Therefore, the preferential location of the spin probe in an aqueous environment that contains both types of polymers is clear: the probe prefers to be in the vicinity of EO groups and reports therefore on the local hydration of these groups.

Based on the a_N values for the probe in PEO, PPO, and the homopolymer mixtures (Figure 5), we added in

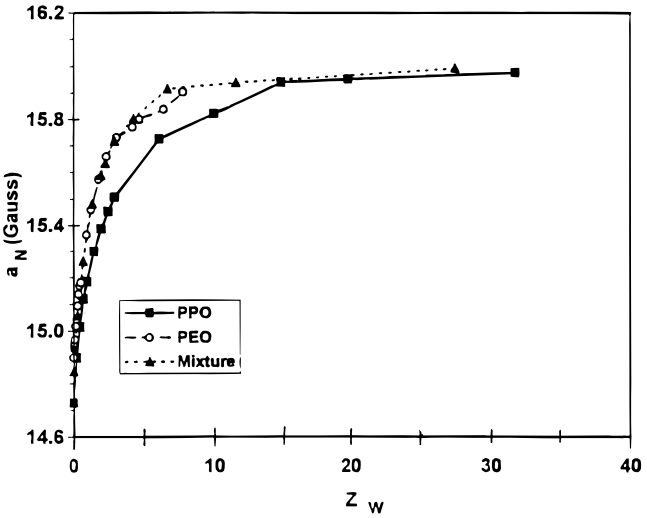

Figure 5. Variation of a_N, the isotropic ^{14}N hyperfine splitting in PDTEMPONE, at 300 K in the indicated aqueous polymer solutions, as a function of Z_w. The polymer mixture is PEO/PPO in the molar ratio 26/30.

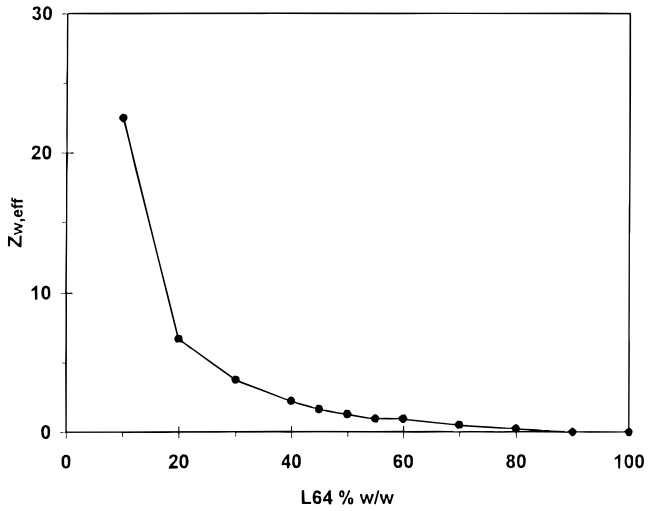

Figure 6. Effective hydration of the EO units in L64, $Z_{w,eff}$, as a function of L64 content, deduced from the calibration curves presented in Figure 5 (see text).

Figure 4 four horizontal scales expressed not in terms of L64 content but in terms of Z_w; the Z_w values are indicated for 0%, 20%, 50%, 70%, 90%, and 100% (w/w) L64. The top additional horizontal scale, Z_w(EO), was calculated from the amount of water in the L64 solutions by assuming that the water is associated with the EO units only. The next scale, Z_w(EO + PO), was calculated with the assumption that the water in the L64 solutions is associated with the EO *and* PO units. The third and fourth scales, Z_w(PDTEMPONE in PEO) and Z_w(PDTEMPONE in mixture), respectively, were deduced by reading the Z_w values corresponding to the a_N values measured experimentally for the above L64 solutions from the curves for PEO and the PEO/PPO mixture given in Figure 5; these scales are the same within experimental error and represent the *effective* hydration of EO units in the L64 solutions. Comparison of the four additional horizontal scales given in Figure 4 in terms of Z_w suggests that at all polymer concentrations the *effective* hydration of the EO units in L64 solutions is significantly lower compared to the hydration calculated from the composition of the solutions containing the spin probe (top two additional scales in Figure 4), even if we assume that the water is associated with the PEO *and* PPO blocks (second from top additional scale in Figure 4). For instance for the L64 solution containing 50% (w/w) polymer, the values of Z_w(EO) and Z_w(EO+PO) are respectively 6.2 and 2.9. The effective hydration is read from Z_w(PDTEMPONE in PEO) and Z_w(PDTEMPONE in mixture), both of which are only 1.3.

The "calibration" curves given in Figure 5 suggest therefore two conclusions: (a) the spin probe is located near the EO units and (b) the corresponding effective hydration value $Z_{w,eff}$ can be read from the calibration curves. The effective degree of hydration $Z_{w,eff}$ of the EO units indicated by the spin probe as a function of L64 content is shown in Figure 6, where the Z_w values are median values of Z_w read from the two bottom horizontal scales shown in Figure 4.

Effect of Temperature. In Figure 7 we present the temperature variation of a_N for the spin probe in L64 solutions, in the temperature range 293−330 K. At a given temperature, a_N decreases with increasing L64 content, as described for the data at 300 K (Figure 2

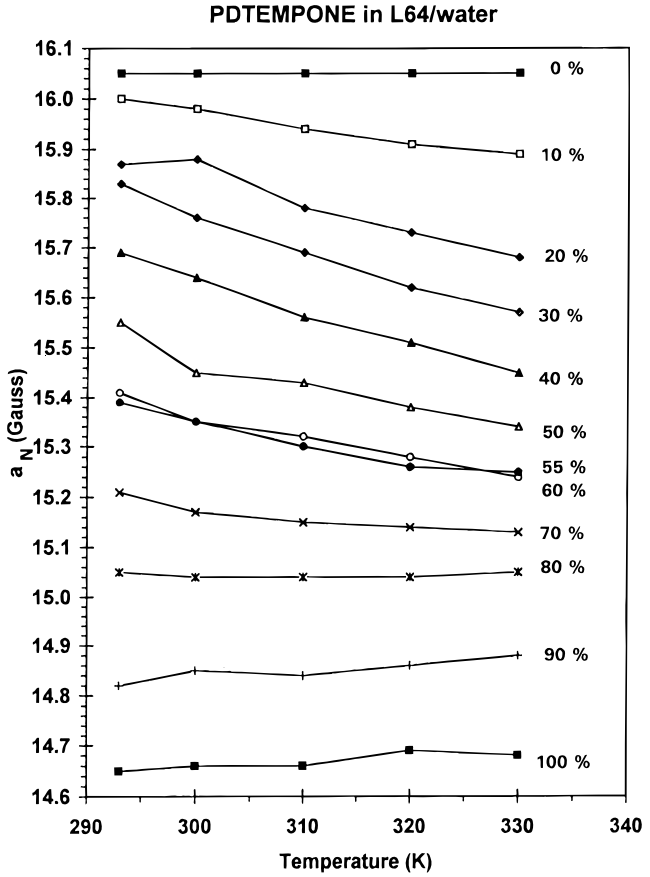

Figure 7. Effect of temperature on a_N, for the indicated L64 concentrations in % (w/w).

and Table 1). The variation of a_N with temperature for a given polymer concentration is in most cases a decrease of a_N, and the decrease is more pronounced in the region of the L_1 phase (10−30% (w/w) L64) and for the solution containing 40% (w/w) L64. The small difference between the a_N values for the 55% and 60% (w/w) L64 is within the experimental error. The slight increase of a_N with temperature for the 90% L64 solution and the pure polymer is difficult to interpret and might be a complication arising from the presence of two spectral components, as seen in Figure 2.

The rotational correlation time τ_c of the probe, for the case of isotropic motion coupled with near-axial sym-

Table 2. Rotational Correlation Times τ_c (s/rad, $\times 10^{11}$) of PDTEMPONE in L64 Aqueous Solutions

% (w/w) L64	293 K	300 K	310 K	320 K	330 K
0	2.5	2.6	1.9	1.8	2.0
10	2.9	3.2	7.2	9.5	12.8
20	5.6	7.1	10.8	13.2	14.8
30	3.9	12.0	13.4	12.7	12.7
40	22.7	16.2	14.7	12.7	12.0
50	21.8	18.6	12.9	12.5	9.9
55	25.6	22.8	15.9	11.4	8.4
60	29.4	24.8	17.3	13.0	7.8
70	34.8	24.7	15.9	10.6	8.0
80	47.4	26.7	16.8	10.1	6.6
90	35.3	26.1	11.6	7.6	5.1
100	31.9	24.6	11.7	7.2	5.5

metry of the hyperfine interaction tensor, can be calculated from eq 2:[31]

$$\tau_c\,(\text{s/rad}) = 1.0238\cdot10^{-6}\,\Delta H_0[(h_0/h_{+1})^{1/2} + (h_0/h_{-1})^{1/2} - 2]/[g_{iso}(A_{\parallel} - A_{\perp})^2] \quad (2)$$

where ΔH_0 is the line width of the central line in **G**, h_{+1}, h_0, and h_{-1} are the heights of the lines corresponding to the ^{14}N nuclear quantum numbers $m_I = 1, 0, -1$, respectively, and $A_{\parallel}$ and $A_{\perp}$ are the ^{14}N hyperfine tensor components in **G**. The factor $1.0238\cdot10^{-6}$ (in G·s/rad) is necessary for conversion of units, from gauss to angular frequency units, $\omega = 2\pi\nu$. The value of g_{iso} is 2.0068.[32,33] The parallel and perpendicular hyperfine tensor components $A_{\parallel}$ and $A_{\perp}$ introduced in eq 2 were deduced from the tensor components for TEMPONE in single crystals of the reduced TEMPONE matrix ($A_{xx} = A_{yy} = 6.6$ G, $A_{zz} = 33.0$ G, leading to $a_{iso} = 15.4$ G) as a standard, by scaling to the experimental isotropic ^{14}N splitting constant a_N of the PDTEMPONE spin probe in each L64 solution measured (Table 1).[32−34]

The correlation times τ_c of PDTEMPONE calculated from eq 2 are presented in Table 2 as a function of temperature and L64 concentration in water. When the temperature increases from 293 to 330 K, the correlation time τ_c remains essentially constant in water, increases in the 10% and 20% (w/w) L64/water solutions, reaches a weak maximum at 310 K in the 30% (w/w) L64/water solution, and decreases in 40%, 50%, 55%, 60%, 70%, 80%, and 90% (w/w) L64/water solutions and pure L64. The general trend for the solutions with the higher polymer content is a decrease of τ_c with increasing temperature; an opposite trend is observed for the solutions corresponding to the micellar (L_1) phase (10%, 20%, and 30% (w/w) L64), where τ_c increases with increasing temperature.

Information on the dynamics of the spin probes can also be obtained by the following semiquantitative approach. The peak-to-peak derivative line width ΔH (in G) of each of the three components in the ESR spectra can be fitted by the expression $\Delta H(m_I) = A + Bm_I + Cm_I^2$, where m_I is the nuclear quantum number that identifies the transition: $m_I = 1, 0, -1$ for the low-field, central field, and high-field transitions.[35] The *A*, *B*, and *C* values can be calculated from the peak-to-peak amplitudes and the line width of the central line, using the inverse proportionality between the line width and the square root of the amplitude. If the magnetic parameters are fixed, and the mechanism of the rotational mobility is identical, the *C* vs *B* dependence is expected to be linear, and the distance of a given point in the plot from the origin should increase monotonically with the correlation time.[35]

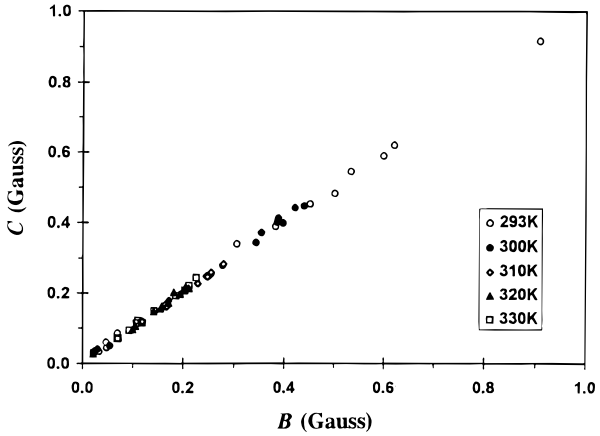

Figure 8. Plot of the parameters *C*(**G**) vs *B*(**G**) determined from the experimental ESR spectra of PDTEMPONE in the L64 solutions, in the temperature range 293−330 K.

In Figure 8 we present the *C*(**G**) vs *B*(**G**) dependence for the spin probe, calculated from the ESR spectra measured as a function of L64 content in the temperature range 293−330 K.[36] The linear dependence shown in Figure 8 suggests that the motional mechanism of the probe is the same across the phase diagram of L64/water. In general, two sets of τ_c values can be calculated, from the *C* and *B* values; if the *C* and *B* values are the same, the two sets of τ_c values are also the same, and the motion of the probe is essentially isotropic.[37] The slope of the *C* vs *B* in Figure 8 is very close to unity, suggesting that the reorientation of the spin probe is isotropic.

Translational Diffusion of PDTEMPONE in L64. Three-dimensional spatial−spectral-intensity perspective plots of the initial images and final images (when a homogeneous distribution of the spin probe in L64 is achieved) are given in Figure 9A,B for the 20% and 90% (w/w) L64/water solutions, respectively. We chose to present these systems because of the contrast in the corresponding images. The progress of diffusion along the spatial coordinate L for the 20% (w/w) solution is observed even for the initial image (Figure 9A, taken 10 min after sample preparation); a sharper front is seen in the more concentrated solution (Figure 9B). The spectral component is also different for the two concentrations: the high-field signal has a lower amplitude in the final image for the more concentrated solution (Figure 9B). These effects are due to different diffusion coefficients and local viscosities, respectively, for the different polymer contents.

The experimental, experimental splined, and simulated concentration profiles for PDTEMPONE in 20% (w/w) L64/water are given in Figure 10, for images taken at times of 10, 60, 160, 235, 290, 350, 810, and 1580 min (final image). The translational diffusion coefficients for PDTEMPONE in L64/water at 300 K are $3.8\cdot10^{-6}$, $6.8\cdot10^{-7}$, $2.1\cdot10^{-7}$, $1.5\cdot10^{-7}$, $9.0\cdot10^{-8}$, and $2.5\cdot10^{-8}$ cm^2 s^{-1} in L64 concentrations of 20%, 40%, 50%, 70%, 90%, and 100% (w/w). The value of *D* for PDTEMPONE in pure water, $1.0\cdot10^{-5}$ cm^2 s^{-1}, was obtained from the diffusion coefficients of the same probe measured by ESRI at 300 K in a series of cross-linked gels with various water contents, by extrapolating to zero network density.[23] The diffusion coefficients are plotted as a function of polymer concentration in Figure 11. Also shown in Figure 11 are the diffusion coefficients of L64 chains in the corresponding aqueous solutions, measured by field gradient NMR.[38]

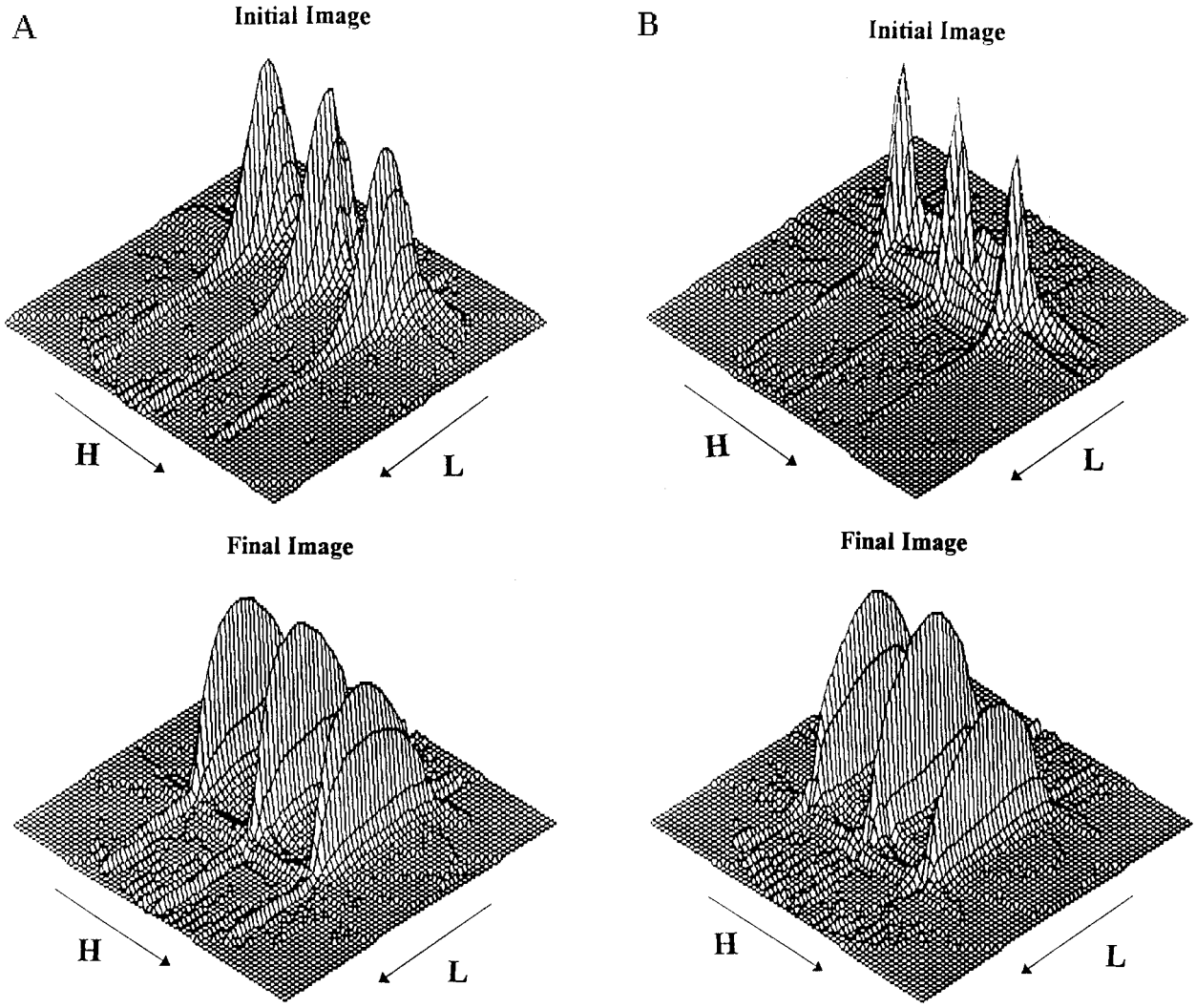

Figure 9. Perspective plots of the three-dimensional spatial−spectral−intensity images for the diffusion of PDTEMPONE at 300 K in 20% (w/w) L64 (A) and 90% (w/w) L64 (B). The length range is 8 mm, and the magnetic field range is 50 G.

Discussion

In this section we will discuss the significance of the results obtained in this study in terms of probe location and local ("effective") hydration, provide details on the micellization process from the temperature and concentration dependence of the magnetic and dynamic parameters of the spin probe, and suggest a mechanism for the translational diffusion of the probe as a function of polymer content.

Probe Location and Effective Hydration. The association of the spin probe with the EO segments was deduced in this study from the "calibration" curves, by comparing the a_N values of the probe in the L64 solutions (Figure 2) with the a_N values measured as a function of the water content Z_w in aqueous solutions of PEO, PPO, and PEO/PPO mixtures (Figure 5). The critical deduction was the preferential solvation of the probe in the vicinity of the EO units. This conclusion must be considered in view of the phase behavior of aqueous PEO/PPO solutions.[39] The experimental phase diagram for PEO600/PPO400/water at 298 K exhibits single phase regions at low polymer contents (below ≈50% (w/w)) and at high polymer contents (above ≈85% (w/w)), irrespective of the PEO/PPO ratio. Between these two limits, the system displays a closed immiscibility region; the corresponding tie lines indicate that the PEO-rich phase contains more water, compared to the PPO-rich phase. Data at 326 K indicate a similar situation, but the two-phase region is more extensive and includes a significant portion of the PPO/water side of the phase diagram. Although the molecular weight of PEO used in our work was lower, 300 vs 600 in ref 38, the main features of the phase diagram are expected to be similar.

The compositions of the PPO/PEO aqueous mixtures investigated in this study encompassed both one- and two-phase regions of the PEO/PPO/water phase diagram; indeed, at some compositions we observed the presence of small droplets, indicative of phase separation. The location of the probe near the PEO chains (or in the PEO-rich phase) and away from the PPO chains is due to the hydrophilicity of the probe. The variation of a_N with L64 content is therefore a reflection of the local polarity and degree of hydration.

In a recent ^1H and ^2H NMR study of the spin−lattice relaxation time T_1 and spin−spin relaxation time T_2 for protons and deuterons in aqueous PEO solutions,[40] Lüsse and Arnold deduced that the number of *bound* water molecules per EO repeat unit is 1. Applying this result to the L64 solutions, we can assume that when $Z_{w,eff} = 1$, all water molecules associated with the PEO groups are bound; this situation occurs for an L64 content of 55% (w/w), and a_N = 15.38 G, as seen in Figure 6. Our results suggest therefore that for L64

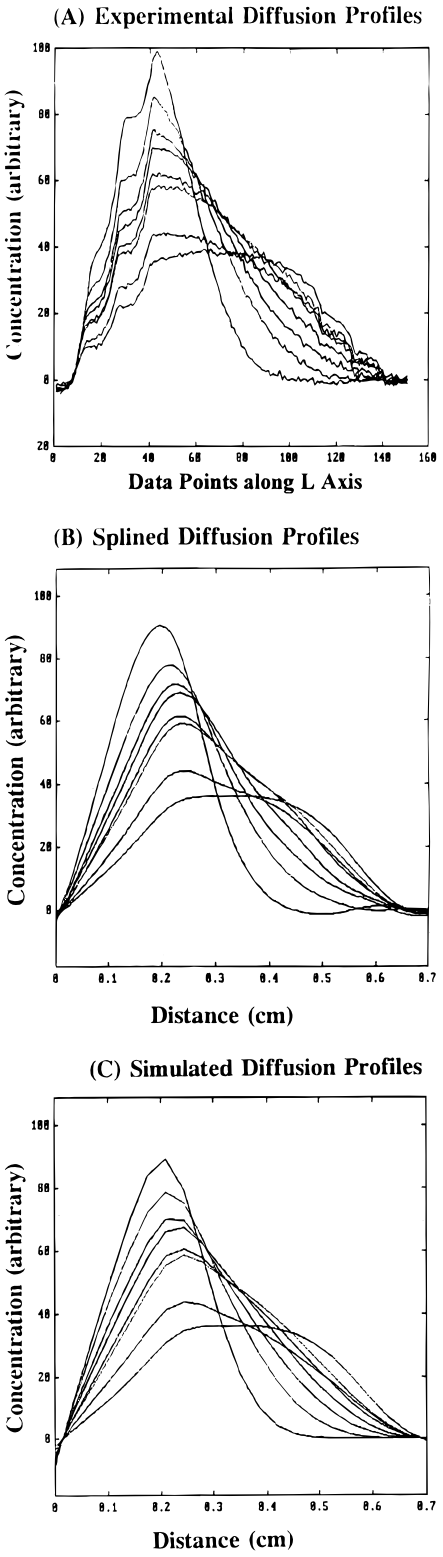

Figure 10. Complete set of experimental (A), experimental splined (B), and simulated (C) concentration profiles for the diffusion of PDTEMPONE in 20% (w/w) L64/water at 300 K. Consecutive experimental images were collected at $t = 10$, 60, 110, 150, 235, 290, 350, 810, and 1580 min (final image).

concentrations < 55% (w/w), both *bound* and *bulk* water are present in the aggregates; at and above this concentration, however, only *bound* water exists. The appearance of an additional component with broad lines for pure L64 and the 90% (w/w) solution suggests that at very low water contents there is little drive for phase separation of the EO and PO regions, and the probe is incapable of selecting a preferential location. It appears

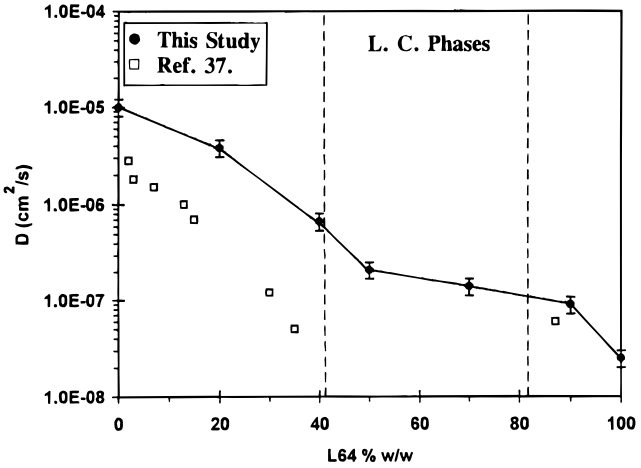

Figure 11. Diffusion coefficients (in $cm^2\ s^{-1}$) as a function of L64 content in the aqueous solutions (●). The experimental points are connected as a guide to the eye. Also presented are the diffusion coefficients of L64 chains measured by pulsed gradient NMR (□).[38]

that the preferential binding of water to the EO units (rather than to the PO units) by hydrogen bonding to the ether oxygen[40] is an important factor in the self-assembling process of the copolymer chains.

Micellization Process. Different methods, such as static and dynamic light scattering, surface tension, dye solubilization methods, and fluorescence, have been used in order to deduce the effects of temperature, polymer concentration, molecular weight, and lengths of the PO and EO blocks on the process of micellization.[4,40] There is no general agreement between the various methods, a conclusion that was at times explained by insufficient temperature control, and/or variations in the structure and polydispersity of the industrial product. The most comprehensive study of the cmc and critical micellization temperature (cmt) has been based on a hydrophobic fluorescent probe, for which the fluorescence efficiency is zero in a hydrophilic environment and unity in a hydrophobic medium.[41] For the specific case of L64, cmc data exist between 303 K (cmc = 1.5% w/v) and 318 K (cmc = 0.02 (w/v)). The cmt values for L64 have also been determined in the concentration range 0.025% (w/v) (cmt = 317.7 K) and 10% (w/v) (cmt = 296.7 K). Another study has reported the presence of aggregates at 298 K only at L64 concentrations above ≈6%.[42]

Details on the micellization process at 300 K can be obtained in this study from the variation of a_N with temperature (Figure 4), the values of $Z_{w,eff}$ across the phase diagram (Figure 6), and the values of the rotational correlation times τ_c of the spin probe (Table 2). It is important to note that the τ_c values can be compared because the analysis of the *C* vs *B* dependence (*vide supra*) suggested that the motional mechanism of the probe is an isotropic rotation across the entire range of L64 concentrations in aqueous solutions. For 10% (w/w) L64, $Z_{w,eff} = 23$ and is similar to the Z_w calculated by assuming that water is distributed evenly between the EO and PO segments. These values suggest that micellization is not significant at 300 K for this concentration. Additional support can be obtained from Table 2: at 300 K, $\tau_c = 3.2 \cdot 10^{-11}$ s/rad, only marginally higher than in pure water at this temperature ($2.6 \cdot 10^{-11}$ s/rad) and for the same polymer solution at 293 K ($2.9 \cdot 10^{-11}$ s/rad). Moreover, the a_N value for this concentration is 15.98 G, only slightly less than the a_N value in pure water at 300 K.

A different situation is evident for the 20% (w/w) L64 solution: a dramatic drop of the effective hydration, from $Z_{w,eff} = 23$ at 10% (w/w) L64 to $Z_{w,eff} = 6.7$ at 20% (w/w) L64, was determined in this study, as seen in Figure 6. The degree of hydration is much lower than the average value calculated on the basis of EO + PO units (11.5) or EO units alone (24.8). The τ_c value (Table 2) is longer by a factor of >2 compared to the value for the 10% (w/w) L64 solution, $7.1 \cdot 10^{-11}$ vs $3.2 \cdot 10^{-11}$ s/rad. These results suggest significant micellization at 300 K in the 20% (w/w) L64 solution, especially compared to the 10% (w/w) L64 solution. The 4-fold increase of τ_c with increasing temperature for the 10% (w/w) L64 solution from 300 to 330 K clearly suggests that micellization occurs at this concentration for $T > 300$ K. The increase of τ_c is not as pronounced for the 20% (w/w) L64 solution and is most likely due to an increase in the size of the aggregates.

A different trend in the τ_c values is observed for L64 contents higher than 30% (w/w): as seen in Table 2, the τ_c values for a given concentration decrease as the temperature increases from 300 to 330 K. Although the macroscopic viscosity of the solution might increase due to aggregate growth, the viscosity sensed by the probe seems to be dominated by the decrease of the *local* viscosity when the temperature increases.

Mechanism of Translational Diffusion. The diffusion coefficients D of the probe (Figure 11) decrease with increasing L64 content in the following manner: significantly in the L_1 phase, slightly in the region of the liquid crystalline phases and the L_2 phase, and significantly again in the pure polymer. The D values for the probe in the isotropic phases follow the general trend observed for the corresponding values of the polymer chains.[38] We observe, however, that the diffusion of the probe is more rapid compared to the polymer chains in the L_1 phase and similar to the polymer chains in the L_2 phase. It seems reasonable to propose that at low polymer contents the probe can diffuse by exchange between the aggregates; the solubility of the probe in water is expected to facilitate this process. At low-water contents, above 80% (w/w) L64, this mechanism is less important, and the probe diffuses together with the polymer chains; as clearly seen in Figure 11, the D values of the probe and the polymer chains are very similar. The strong decrease of the transport rate of the probe for high-L64 contents (≥50% (w/w)) parallels the decrease in the amount of bulk water in the aggregates in the liquid crystalline phases: as deduced above, the amount of bulk water is negligible for polymer contents above 55% (w/w). These trends suggest that the presence and amount of *bulk* water in the aggregates play major roles in determining the diffusion rate of the probe.

An understanding of the diffusion mechanism of a small probe is important for applications that use aggregated Pluronics as drug delivery systems. The transport rates measured in this study suggest that although the small probe is associated with the aggregates, its diffusion is more rapid compared to that of the aggregates at low polymer content because it is soluble in water. When this alternative transport mechanism is not possible, for instance at very low-water contents, the rates of transport of the small probe and the polymer chains are similar, in spite of the difference in the molecular weights.

Conclusions

The isotropic ^{14}N hyperfine splitting of the nitroxide spin probe, a_N, is a key parameter of the local polarity, and its variation with temperature is an indicator of aggregation. The effective hydration of the polymer chains was determined by comparison of a_N values of the probe across the phase diagram, with "calibration" curves of a_N in pure PEO, pure PPO, and mixtures of the homopolymers as a function of water content Z_w, defined as the number of water molecules per monomer unit. The calibration curves indicated that the spin probe is preferentially located in the vicinity of the EO segments and reports on the local polarity and hydration of these segments.

The *effective* degree of hydration $Z_{w,eff}$ is significantly lower than the *average* hydration deduced on the basis of the water content in the L64 solutions and decreases with increase in L64 content. The dramatic drop in $Z_{w,eff}$ at 300 K from $Z_{w,eff} \approx 23$ in 10% (w/w) L64 to $Z_{w,eff} \approx 7$ in 20% (w/w) L64 was taken as an indicator of micellization in the latter solution.

The dependences of a_N and τ_c, the rotational correlation time of the probe, on temperature and L64 content are additional parameters that describe the local polarity and the micellization process. We suggested that at high-polymer contents (≥90% (w/w) L64) the EO and PO blocks are intermingled, leading to separate ESR signals for probes in two different environments.

The diffusion coefficients of the spin probe decrease with increase in the polymer content, but the decrease is more prominent for L64 contents in the range 10−30% (w/w). At a polymer content of 90% (w/w), the diffusion coefficient of the probe is similar to that of the polymer chains (determined by field gradient NMR[38]), in spite of the difference in molecular weights. We proposed that water provides an important pathway for the translational diffusion of the probe.

Acknowledgment. This study was supported by the Polymers Program of the National Science Foundation. The authors are grateful to Jay Otten (BASF) for the gift of the L64 sample, Gary C. Rex (Union Carbide) for the Carbowax samples, Arco Corp. for the PPO sample, and Jiri Labsky (Institute of Macromolecular Chemistry, Prague) for the synthesis of the spin probe used in this study. S. Schlick is grateful to Professor Isao Ando and his group at the Department of Polymer Chemistry, Tokyo Institute of Technology, for their warm hospitality during her sabbatical stay in Tokyo, where this manuscript was finalized.

References and Notes

(1) Israelachvili, J. *Intermolecular and Surface Forces*, 2nd ed.; Academic Press: London, 1991.
(2) *Pluronic and Tetronic Surfactants*; technical brochure; BASF Corp.: Parsippany, NJ, 1989.
(3) Almgren, M.; Brown, W.; Hvidt, S. *Colloid Polym. Sci.* **1995**, *273*, 2.
(4) Alexandridis, P.; Hatton, T. A. *Colloids Surf. A: Physicochem. Eng. Aspects* **1995**, *96*, 1.
(5) (a) Karlstrom, G. *J. Chem. Phys.* **1985**, *89*, 4962. (b) Andersson, M.; Karlstrom, G. *J. Chem. Phys.* **1985**, *89*, 4957.
(6) (a) Linse, P. *Macromolecules* **1993**, *26*, 4437. (b) *J. Phys. Chem.* **1993**, *97*, 13896.
(7) Hurter, P. N.; Scheutjens, J. M. H. M.; Hatton, T. A. *Macromolecules* **1993**, *26*, 5030.
(8) Holland, R. J.; Parker, E. J.; Guiney, K.; Zeld, F. R. *J. Phys. Chem.* **1995**, *99*, 11981.
(9) Zhou, Z.; Chu, B. *Macromolecules* **1987**, *20*, 3089.
(10) Zhou, Z.; Chu, B. *Macromolecules* **1988**, *21*, 2548.
(11) Wu, G.; Zhou, Z.; Chu, B. *Macromolecules* **1993**, *26*, 2117.

(12) Zhou, Z.; Chu, B. *Macromolecules* **1994**, *27*, 2025.
(13) Malmsten, M.; Lindman, B. *Macromolecules* **1993**, *26*, 1282.
(14) Houlihan, P. W.; Fornasiero, D.; Gieser, F.; Healy, T. W. *Colloids Surf.* **1992**, *69*, 147.
(15) Zhang, K.; Khan, A. *Macromolecules* **1995**, *28*, 3807.
(16) Alexandridis, P.; Olsson, U.; Lindman, B. *Macromolecules* **1995**, *28*, 7700.
(17) DiMeglio, J. M.; Paz, L.; Dvolaitzky, M.; Taupin, C. *J. Phys. Chem.* **1984**, *88*, 6036.
(18) Hecht, E.; Mortensen, K.; Hoffmann, H. *Macromolecules* **1995**, *28*, 5465.
(19) Zhou, L.; Schlick, S. *Polym. Prepr. (Am. Chem. Soc. Div. Polym. Chem.)* **1996**, *37*, 829.
(20) Caragheorgheopol, A.; Pilar, J.; Schlick, S. *Macromolecules*, submitted for publication.
(21) Chiarelli, R.; Rassat, A. *Tetrahedron* **1973**, *29*, 3639.
(22) Szajdzinska-Pietek, E.; Schlick, S.; Plonka, A. *Langmuir* **1994**, *10*, 1101, 2188.
(23) Schlick, S.; Pilar, J.; Kweon, S.-C.; Vacik, J.; Gao, Z.; Labsky, J. *Macromolecules* **1995**, *28*, 5780.
(24) Kweon, S.-C. M.S. Thesis, University of Detroit Mercy, Detroit, MI, 1993.
(25) Maltempo, M. M.; Eaton, S. S.; Eaton, G. R. In *EPR Imaging and In Vivo EPR*; Eaton, G. R., Eaton, S. S., Ohno, K., Eds.; CRC Press: Boca Raton, FL, 1991; Chapter 13, p 135.
(26) Gao, Z.; Pilar, J.; Schlick, S. *J. Phys. Chem.* **1996**, *100*, 8430.
(27) Kruczala, K.; Gao, Z.; Schlick, S. *J. Phys. Chem.* **1996**, *100*, 11427.
(28) Gao, Z.; Schlick, S. *J. Chem. Soc. Faraday Trans.* **1996**, *92*, 4239.
(29) Crank, J. *The Mathematics of Diffusion*; Clarendon Press: Oxford, U.K., 1993.
(30) The degree of polymerization has a slight effect on the a_N value: a_N for PDTEMPONE in Carbowax 600 (13 EO units, as one of the blocks in L64) is 14.81 G, compared to 14.90 G in Carbowax 300 (6 EO units).
(31) Noel, C.; Lauprêtre, C.; Friedrich, C.; Leonard, C.; Halary, J. L.; Monnerie, L. *Macromolecules* **1986**, *19*, 201. The expression for the rotational correlation time τ_c, eq 1, is appropriate for isotropic tumbling but is expected to be a good approximation for the *average* value of τ_c in the case of anisotropic motion, such as that for the liquid crystalline phases in L64.
(32) *Spin Labeling. Theory and Applications*; Berliner, L. J., Ed.; Academic Press: New York, 1976; p 554.
(33) Snipes, N.; Cupp, J.; Cohn, G.; Keith, A. *Biophys. J.* **1974**, *14*, 20.
(34) Szajdzinska-Pietek, E.; Pilar, J.; Schlick, S. *J. Phys. Chem.* **1995**, *99*, 313.
(35) Pilar, J.; Labsky J.; Schlick, S. *J. Phys. Chem.* **1995**, *99*, 12947 and references therein.
(36) The value of B deduced on the basis of m_I values is negative. In Figure 8 we plotted the absolute value of B.
(37) Marsh, D. In *Biological Magnetic Resonance, Vol. 8*; Berliner, L. J., Reuben, J., Eds.; Plenum Press: New York, 1989; Chapter 5, p 261.
(38) Zhang, K.; Lindman, B.; Coppola, L. *Langmuir* **1995**, *11*, 538.
(39) Malmsten, M.; Linse, P.; Zhang, K. *Macromolecules* **1993**, *26*, 2905.
(40) Lüsse, S.; Arnold, K. *Macromolecules* **1996**, *29*, 4251.
(41) Alexandridis, P.; Holzwarth, J. F.; Hatton, T. A. *Macromolecules* **1994**, *27*, 2414.
(42) Al-Saden, A. A.; Whateley, T. L.; Florence, A. T. *J. Colloid Interface Sci.* **1982**, *90*, 303.

MA961321R